STABILITY ANALYSIS OF ANTI-ISLANDING PROTECTION BASED ON POSITIVE FEEDBACK TECHNIQUE

Andrei Giordano Holanda Battistel[1], Igor Weide Jaskulski[2], Humberto Pinheiro[2]

[1]Dept. of Electrical Eng./COPPE
Federal University of Rio de Janeiro
Rio de Janeiro, RJ – Brazil

[2]Power Electronics and Control Research Group (GEPOC),
Federal University of Santa Maria
97105-900 Santa Maria, RS – Brazil

andrei.battistel@gmail.com igorwj@gmail.com humberto.ctlab.ufsm.br@gmail.com

***Abstract* – This paper develops a stability analysis of a local Islanding Detection Algorithm (IDA) based on positive feedback technique that has no Non Detection Zone (NDZ). A complete dynamic model for the system is derived and the stability analysis with Nyquist stability criterion is carried out. It is demonstrated that the parameters of the IDA can be easily tuned at the key operating conditions to guarantee the under or over voltage relay tripping whenever islanding occurs. Finally, experimental results are presented to support the theoretical analysis developed.**

***Keywords* - Anti-islanding, Loss of Mains, Distributed Generation (DG), Stability Analysis.**

I. INTRODUCTION

The electric energy demand is growing constantly in the last decades. The forecast of the electric energy demand in the world in 2030 is twice the consumption of 2003 [1]. There are many options to attend this demand, among them is highlighted the use of distributed generation (DG). The appealing factors of DG are [2]: (i) DG units are usually connected close to consumers so that the distribution and transmission losses and costs are reduced or even avoided; (ii) it is easier to find sites for small generators and; (iii) the liberalization of the electricity market contributes to create opportunities for new enterprising in the power generation sector through investments in DG units.

It is important to mention that distribution systems have been for decades designed considering power and currents flowing from substations to the loads. As a result, the integration of DGs at traditional distribution systems meets with issues and obstacles in aspects as protection, stability, energy market structure, etc. The condition called Islanding is among these obstacles.

Islanding is a condition at which a section of the network including a DG unit is disconnected from the main grid and, during the period of disconnection, the DG continues to supply active and reactive power to local load with reasonable voltage and frequency. Figure 1 shows an islanding scenario.

Unintentional islanding is a concern because it may result in energy-quality issues, interference to grid-protection devices, damage to power generation and utility as a result of unsynchronized re-closure as well as personnel safety hazards [3].

The *Std* IEEE 1547 [4] is a series of standards that gives specifications and technical requirements for the interconnection of distributed generators with aggregate capacity of 10 MW or less. The section 4.4 of *Std* IEEE 1547 points that the DG interconnection system shall detect the islanding condition and cease to energize the islanded section within two seconds after the island formation. Therefore, a DG must have a device or equipment that detects the islanding condition within the time limits specified.

The performance of an Anti-Islanding device or equipment can be evaluated by the Non Detection Zone (NDZ). The NDZ defines a region in ΔP and ΔQ space where the IDA fails, where ΔP and ΔQ are the active and reactive power mismatch between DG and local load (consumers), respectively [5]. So, a small or null NDZ is desirable.

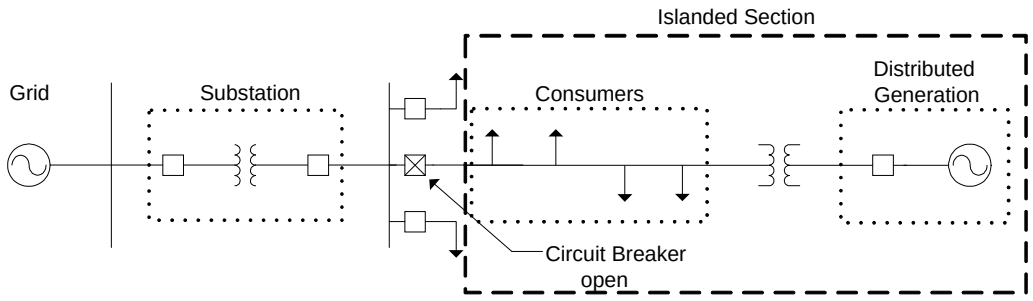

Figure 1. Scenario with an islanded section

Artigo submetido em 14/09/2011. Aceito para publicação em 23/11/2011
por recomendação do editor João Onofre P. Pinto.

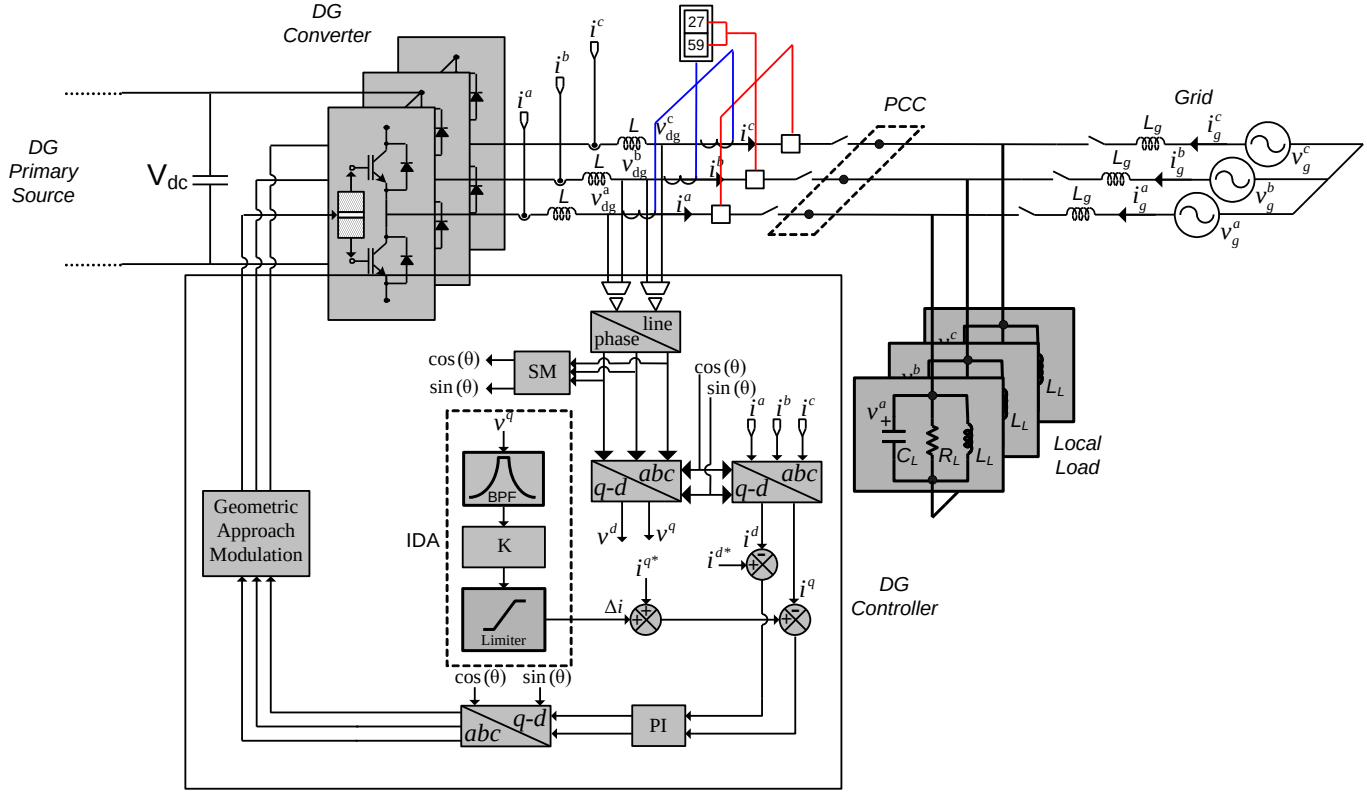

Figure 2. Block Diagram of a DG with the Islanding Detection Algorithm (IDA) connected in a distribution system

The IDAs can be classified in two groups: remote and local.

The remote techniques detect the opening of contacts at the point of disconnection and transmit that signal to all DGs that could supply the respective islanded zone. Usually, remote methods have no NDZ, but as they are based on communication between the grid and DGs, these techniques tend to be expensive compared to the local ones [6].

The local techniques are based on the information available at DG site. Normally, this information is available as part of DG control systems, so additional sensors and components are not required. Therefore, the implementation costs are usually low. The drawbacks of local techniques are the presence of NDZ and the power quality degradation with the current harmonics injection [6-8].

An interesting review on IDAs for distributed generation can be seen in [9], where different existing techniques are presented and compared. It is also important to note that this has been a subject of recent efforts. Indeed, several recent papers dealing with IDAs have been published, for instance the references [10-12], where new techniques are proposed as well as concerns related to the NDZ issue.

One of these methods was proposed by Ye at al [13], where a local technique that has no significant impact on PCC voltage THD and has no NDZ is shown. This algorithm is based on positive feedback that drives away the limits of voltage or frequency when the utility section, where the DG is operating, is islanded.

IDAs with positive feedback loop should be stable when the grid is present and unstable when islanded. It means that whenever the grid is not present, a voltage oscillation must occur in the DG output. Consequently, the under/over voltage relays can be adjusted to trip whenever islanding occurs. Therefore, a discerning stability analysis for these algorithms should be developed to ensure the right operation of islanding detection. So far, this analysis has not been reported in the literature.

This paper proposes a stability analysis of the scenario shown in Figure 2 under the following conditions: (i) DG without the IDA when the grid is present; (ii) DG without the IDA when the grid is not present; (iii) DG with the IDA when the grid is present and; (iv) DG with the IDA when the grid is not present.

From the analysis carried out, it is demonstrated that the parameters of IDA can be easily tuned to meet the grid code requirements. In addition, an estimation for under/over voltage relays coordination is shown.

The remainder part of this paper is organized as follow: Section II describes the DG unity, the local load, the equivalent grid and the IDA. Section III analyzes the stability for the four conditions. In order to validate the stability analysis as well as the numerical simulation results, section IV presents the experimental results. Finally section V shows the conclusions.

II. SYSTEM DESCRIPTION

The circuit where the stability analysis is performed is shown in Figure 2. The DG system, the local load, the equivalent grid and the IDA are described in this section.

A. DG System

For the purpose of this study, the DG is considered to be connected to the grid by means of a three-phase PWM converter, Figure 2, where DC bus is constant and the output filter is comprised by an inductor *L*. This simplification is valid because usually DG power-conditioning systems include a regulated DC source, an output filter and an interconnection transformer which are usually strongly inductive. The DG control method as well as the DC/AC converter topology are described in [14].

The synchronization method with the grid (SM block in Figure 2) is based in a passive band-pass filter with low cut-off frequency that will be described in the next section.

B. Synchronisation Method

There are a number of methods to synchronize the PWM converter with the grid [15-16]. Here, a simple method based on two band-pass filters is used, as shown in Figure 3. In [17], the authors propose a method based on low-pass filters. However, it has found experimentally that this method is quite sensitive to DC components present in the measured voltages. Considering that is arduous to take out entirely the DC level in the measurements in an experimental setup, the low-pass filters have been replaced by second order band-pass filters (BPF) with cut-off frequency of 5 Hz. In addition, a low-pass filter on the voltage norm has been included to remove the undesired 120 Hz component resulted from voltage unbalance.

Finally, a rotation matrix *R* is used to compensate the phase lag of the BPF filters, which is given by:

$$\mathrm{R}(\Delta\theta)=\begin{bmatrix}\cos(\Delta\theta) & -\sin(\Delta\theta)\\ \sin(\Delta\theta) & \cos(\Delta\theta)\end{bmatrix} \quad (1)$$

where $\Delta\theta$ is the BPF phase lag at the grid frequency. In the present case, $\Delta\theta$=84.23 rad/s .

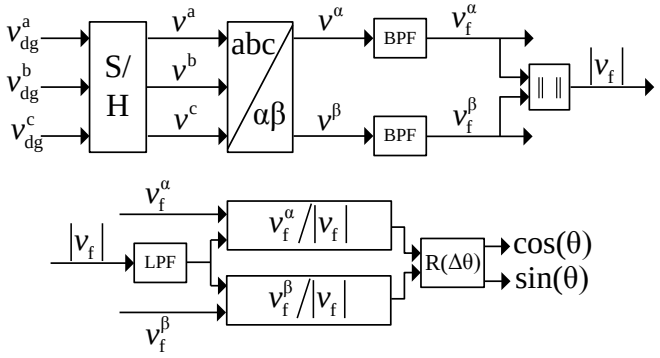

Figure 3. Block diagram of the synchronization method (SM)

C. Local Load and Grid

The *Std* IEEE 1547.1 [18] specifies a test procedure for islanding detection equipment. The test circuit defined in this procedure is shown in Figure 4.

The capacitance C_L and inductance L_L are as follows:

$$C_L=\frac{PQ_f}{2\pi f v^2} \quad (2)$$

$$L_L=\frac{v^2}{2\pi f P Q_f} \quad (3)$$

where

P - DG active output power per phase (W)

f - grid frequency (Hz)

v - nominal phase voltage across each phase of the *RLC* load (V)

Q_f - quality factor of the parallel (*RLC*) resonant load that is given by

$$Q_f=R_L\sqrt{\frac{C_L}{L_L}} \quad (4)$$

The resistance R_L is calculated as

$$R_L=\frac{v^2}{P} \quad (5)$$

In addition, the local load parameters must be obtained for $Q_f=1\pm0.05$.

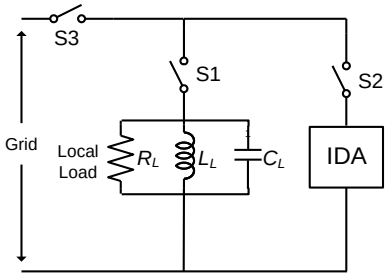

Figure 4. Unintentional islanding test configuration

The substation feeder and the grid of Figure 1 are represented as an infinite bus with an equivalent inductance L_g, as shown in Figure 2. The *Std* IEEE 1547 establishes that the minimum short-circuit current in the PCC where the DG is connected must be

$$I_{ccmin}=20I_n \quad (6)$$

where I_n is DG rated current of one phase.

Therefore, the maximum of L_g is given by

$$L_{gmax}=\frac{v}{I_{ccmin}2\pi f} \quad (7)$$

Usually, there is a power transformer between the PCC and the DG that steps up the output DG voltage. So, it is convenient to reflect the L_{gmax} to the transformer low-voltage side, i.e.:

$$L^L_{gmax}=\frac{1}{\alpha^2}L_{gmax} \quad (8)$$

where α is the voltage transformation ratio.

Table I shows the parameters of local load and grid used for the analysis.

TABLE I

Parameters of Local Load and Grid

Parameter	Value	Parameter	Value
L	1.125 [mH]	L^L_{gmax}	19.15 [μH]
C_L	551.2 [μF]	$v^a_g=v^b_g=v^c_g$	24.5 [V_{rms}]
L_L	12.8 [mH]	ω_0	6.283 [rad/s]
R_L	4.812 [Ω]	Q	2

D. Islanding Detection Algorithm (IDA)

The active IDA block diagram considered in this paper is shown in Figure 2. In this system, the voltages in abc stationary frame are measured and transformed to q-d synchronous frame resulting in the components v^q and v^d. The component v^q is filtered by a second order band-pass filter (BPF) and then it is multiplied by a gain K. This signal passes through a saturation limiter resulting in Δi, which is added to a current reference i^{q*}. Qualitatively the IDA operation can be explained considering a positive feedback loop. When the DG output voltage is increasing, the IDA will command the DG output active power to be increased. Due to the local load characteristic, the DG output voltage will also increase to balance the active power. As a result, the DG output voltage will increase up to defined voltage limits and therefore, the islanding can be detected by the over/under voltage relays.

Quantitatively is possible to estimate the frequency and the amplitude of a possible limit cycle associate with the IDA by modeling the non-linear saturation function, present in the considered IDA, by its describing function. These estimated values are useful for the over/under voltage relays coordination.

III. SYSTEM STABILITY ANALYSIS WITH THE ISLANDING DETECTION ALGORITHM

In order to investigate the impact of the considered IDA in the DG control system, a stability analysis is carried out in this section. To perform such analysis, a complete model in *q-d* synchronous frame of the system shown in Figure 2 is derived.

A. Dynamic Models

Figure 5 shows the dynamic model in q-d synchronous frame of Figure 2 where u^q and u^d represent the three DG converter output voltages; v^q_g and v^d_g represent the three grid voltages; i^q and i^d represent the three DG converter output currents; i^q_g and i^d_g represent the three grid currents; i^q_L and i^d_L represent the three currents through local load inductance; and, finally, ω is the grid frequency in rad/s.

Considering that this dynamic model represents a MIMO system where u^q and u^d are dependent on grid voltages and currents reference, a state-variable model is suitable.

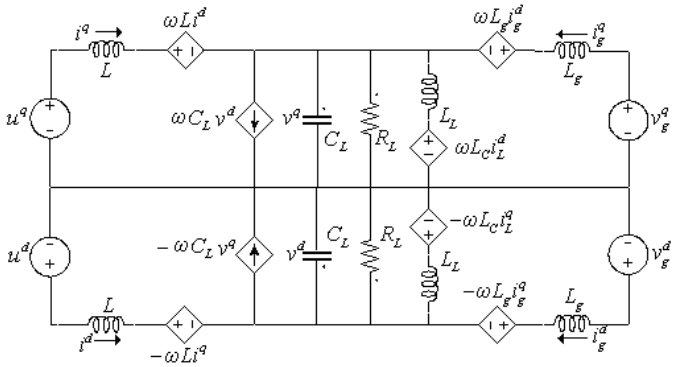

Figure 5. Complete Dynamic Model

An examination of Figure 5 reveals that the dynamic model can be described by a state equation with eight states in q-d coordinates. Besides, the state equations of the PI controller and the BPF of IDA must be considered in order to achieve a full system model.

The two PI controllers of Figure 2 can be described as:

$$\begin{bmatrix}\dot{x}_{PI1}\\ \dot{x}_{PI2}\end{bmatrix}=\begin{bmatrix}0 & 0\\ 0 & 0\end{bmatrix}\begin{bmatrix}x_{PI1}\\ x_{PI2}\end{bmatrix}+\begin{bmatrix}1\\ 1\end{bmatrix}\begin{bmatrix}i^{q*}-i^q\\ i^{d*}-i^d\end{bmatrix} \tag{9}$$

$$\begin{bmatrix}u^q\\ u^d\end{bmatrix}=\begin{bmatrix}K_{INV}K_I & 0\\ 0 & K_{INV}K_I\end{bmatrix}\begin{bmatrix}x_{PI1}\\ x_{PI2}\end{bmatrix}+\begin{bmatrix}K_{INV}K_P & K_{INV}K_P\end{bmatrix}\begin{bmatrix}i^{q*}-i^q\\ i^{d*}-i^d\end{bmatrix} \tag{10}$$

Similarly, the BPF of IDA can be described as state space equation:

$$\begin{bmatrix}\dot{x}_1\\ \dot{x}_2\end{bmatrix}=\begin{bmatrix}-\omega_n & -\omega_n^{\,2}\\ 1 & 0\end{bmatrix}\begin{bmatrix}x_1\\ x_2\end{bmatrix}+\begin{bmatrix}1\\ 0\end{bmatrix}\begin{bmatrix}v^q\end{bmatrix} \tag{11}$$

$$\begin{bmatrix}\Delta v\end{bmatrix}=\begin{bmatrix}K\dfrac{\omega_n}{Q} & 0\end{bmatrix}\begin{bmatrix}x_1\\ x_2\end{bmatrix}+\begin{bmatrix}0\end{bmatrix}\begin{bmatrix}v^q\end{bmatrix} \tag{12}$$

where Q is the quality factor and ω_n the BPF center frequency.

As a result, the complete model can be represented as:

$$\begin{aligned}\dot{x} &= Ax+Bu\\ y &= Cx+Du\end{aligned} \tag{13}$$

where *x*, *y* and *u* are the states, outputs and the inputs, respectively. *A*, *B*, *C* and *D* depend on the system parameters.

The state equations including the dynamic model of Figure 5 are shown in the appendix.

B. Stability Analysis

For the selection of the IDA parameters is very important to guarantee a stable operation when the DG is connected into the grid and an oscillating operation when the DG is islanded. The BPF cut-off frequency and the gain K can be selected by applying the Nyquist extended criterion. Besides, due to the presence of a non-linearity, the Nyquist extended criterion is an excellent tool of evaluating the limits of IDA saturation to meet a given specific technical requirement.

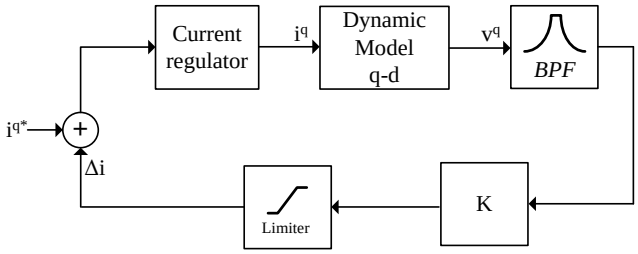

Figure 6. Block diagram to investigate the stabilty

In order to apply Nyquist criterion, a transfer function is derived from the state space model (13). This is possible by evaluating (14) since *A*, *B* and *C* are known. The input i^{q*} and the BPF output are considered, as shown in Figure 6.

$$G(s) = C[sI - A]^{-1}B \tag{14}$$

The IDA parameters values are shown in Table II below:

TABLE II

Islanding Detection Algorithm Parameters

Parameter	Value	Description
K_{INV}	55	DG Converter Gain
Kp	411	Proportional Gain of PI
Ki	0.411	Integral Gain of PI
ω_n	3.14 rad/s	BPF center frequency
Q	2	BPF quality factor
K	1.5	BPFgain
S	2	Saturation limit

The transfer function G(s) is Hurwitz stable at all operating conditions. Therefore, the stability analisys can be evaluated by means of comparing the locus of G(s) with the locus of the saturation negative inverted describing function, that is the locus of -1/N where N is the describing function of the saturation non-linearity [19]. Note that the system is expected to oscillate if there is an intersection between the two loci. Furthermore, this intersection allows the calculation of both the voltage oscillation amplitude and frequency values.

Firstly, the Nyquist plots without IDA are shown for the cases with: (i) grid connected, Figure 7 and (ii) grid disconnected, Figure 8.

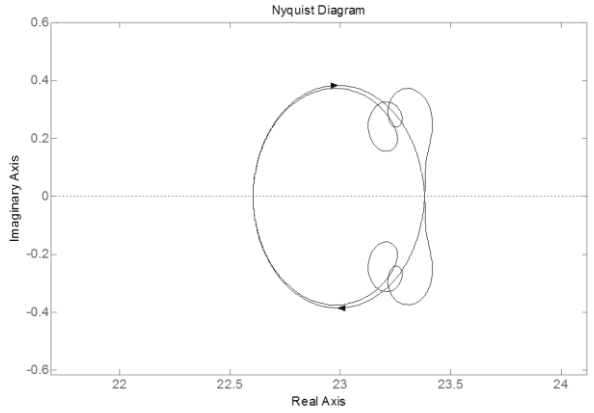

Figure 7. Nyquist plot without IDA with grid connected

Note in Figure 7 and 8 that the overall system is stable for both cases since none of them encircle the critical point -1+j0.

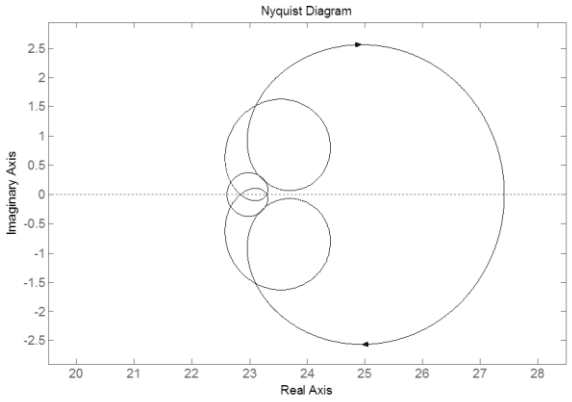

Figure 8. Nyquist plot without IDA for disconnected grid

As expected, the unintentional islanding operation is possible with this configuration. On the other hand, by adding the IDA, the system behavior is not modified significantly when grid is connected; remaining, thus, stable as shown in Figure 9.

However, when the grid is not present, Figure 10, it is possible to observe an intersection between the locus of G(s) and the locus of -1/N plot in the complex plane, which, as mentioned, indicates a possible limit-cycle. Besides, a possible limit-cycle can be predicted due to the loci intersection.

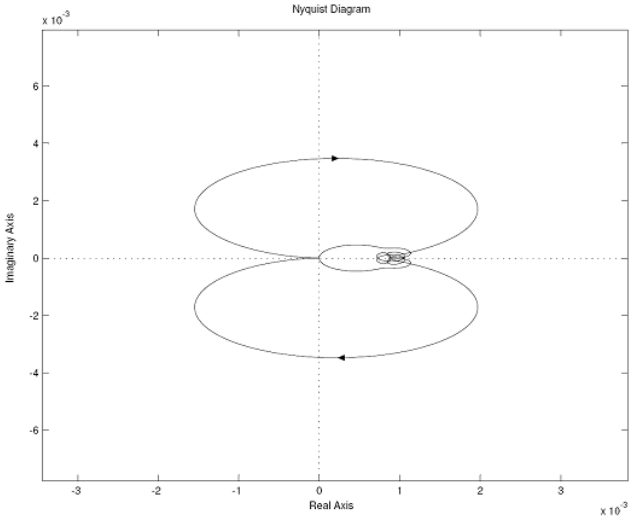

Figure 9. Nyquist plot with IDA for connected grid

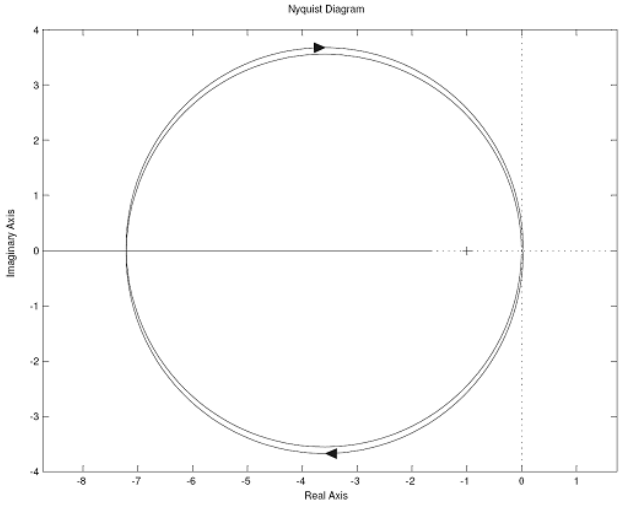

Figure 10. Nyquist plot with IDA for disconnected grid

Figures 7 to 10 show that the initial purpose was satisfied concerning system behavior with or without the IDA and for both connected and disconnected grid. It is important to note here that the amplitude of voltage oscillation and its frequency can be calculated from the Nyquist plot. The frequency can be directly obtained from the intersection point of the loci in the complex plane. In addition, the amplitude of the fundamental at the saturation nonlinearity input, Δv, can be easily obtained since it is related to the describing function gain. As the value of -1/N at the intersection point can be directly obtained from the plot, it is

possible to find Δv. Finally, as Figure 6 indicates, this amplitude is the quadrature axis voltage, v^q, filtered, which means that the magnitude can be obtained dividing Δv by the BPF gain.

The system behavior predicted by the Nyquist criterion will be compared with the numerical simulation results using test condition parameters of Table I, discussed in Section II. Figure 11 shows the inverter output voltage and the grid current. The grid is disconnected at t=4s. It is possible to see that undesirable islanding has been formed. On the other hand, Figure 12 shows a similar case but with the IDA included. It is possible to see an oscillation on the voltage amplitude that can be detected by the under/over voltage relays.

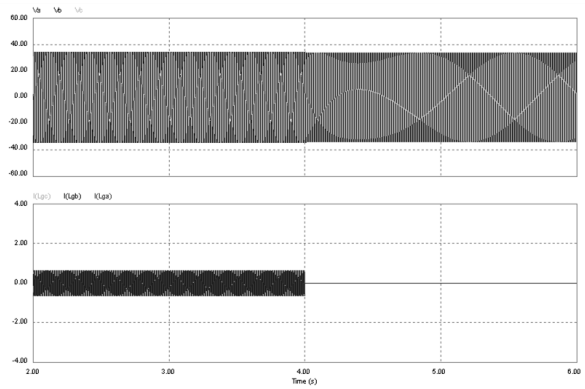

Figure 11. Simulation result without IDA. Top: Inverter output voltage. Bottom: Gird Current

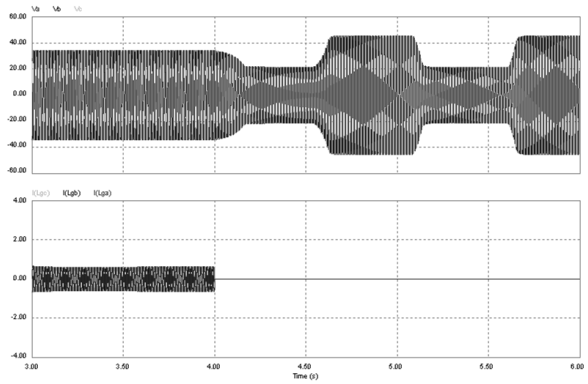

Figure 12. Simulation result with IDA. Top: Inverter output voltage. Bottom: Gird Current

Although these results are in good agreement with the theoretical analysis, the voltage amplitude profile of Figure 12 during the oscillation could be improved. This voltage amplitude profile results from the fact that the output of saturation nonlinearity, which is driven by a sinusoid from the BPF output, is a quasi-square waveform. This is responsible for the square shape seen in DG output voltage of Figure 12. It is unnecessary to say that abrupt variations of voltage may jeopardize both DG and load equipment, being, thus, undesirable. Aiming to solve this problem, a modification in the IDA is proposed.

By adding a band pass filter at the saturation nonlinearity output, the voltage amplitude profile during oscillation is expected to be smoothened. Also, this new component shall not change system stability behavior. The new structure of the IDA is shown in Figure 13.

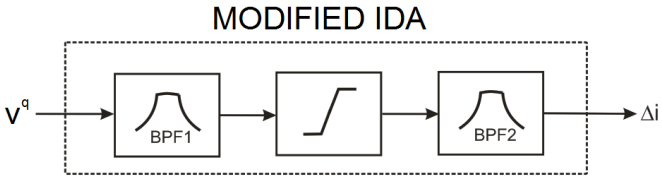

Fig 13. Proposed modification.of IDA

The analysis can be easily carried out by combining G(s) with the new BPF transfer function. Then, the Nyquist plots can be used to infer on the stability. It has been found out that a filter with the same center frequency and Q factor as that of Figure 2 is suitable. As the gain of this filter is related to the amplitude of the oscillation, it can be used to ensure the under/over voltage relays tripping. Figure 14 shows the Nyquist plot for three different BPF gains when the grid is disconnected.

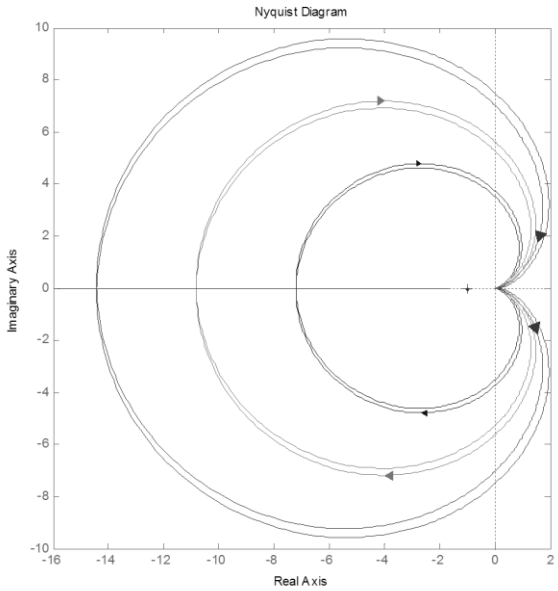

Fig 14. Nyquist plot for three different BPF gains with grid disconnected

TABLE III

Result Comparison of Voltage Oscillation Amplitude

Gain	Mathematical Prediction	PSIM	Error
1	0.1768 p.u.	0.1751 p.u.	0.99%
1.5	0.2657 p.u.	0.2632 p.u.	0.95%
2	0.3546 p.u.	0.3510 p.u.	1.01%
2.5	0.4435 p.u.	0.4391 p.u.	0.99%
3	0.5324 p.u.	0.5270 p.u.	1.02%

From Figure 14 is possible to conclude that: (i) the modified system is capable of operating as desired; (ii) the filter gain can be tuned to result in the desirable amplitude values and; (iii) there is an almost linear relationship between the gain of BPF and the voltage oscillation amplitude. In order to demonstrate the accuracy of the analysis carried out, Table III compares the amplitude predicted by mathematical

models and those obtained from numerical simulation for different BPF2 gain values. All other parameters are kept unchanged. Values are given in per-unit referred to the nominal line voltage.

Indeed, these numbers confirm a quite linear relationship between voltage amplitude oscillation and BPF2 gain. In addition, the differences between the amplitudes of the oscillations predicted and ones obtained by numerical simulations are under 1%. Simulation results with this modification are seen in Figure 15, where it is possible to note that the oscillation profile is indeed smoothened by the addition of a second BPF.

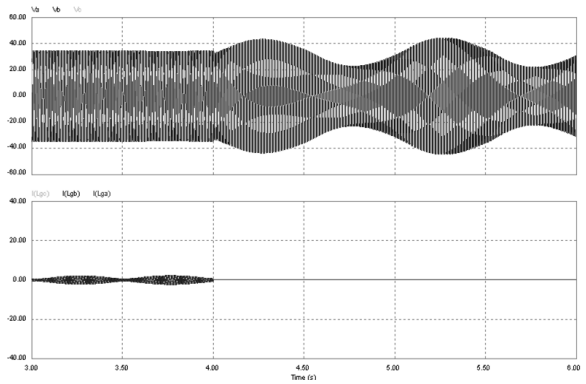

Fig 15. Simulation result with BPF addition

It is worth mentioning that in the first case, with just one BPF, the saturation limit is the main responsible for the voltage oscillation amplitude. However, with the addition of the second, BPF2, this voltage oscillation amplitude can be defined by its gain. Furthermore, the BPF cut-off frequencies determine the oscillation frequency. Thus, it is possible to coordinate under/over voltage relays accordingly to the time specification of IEEE 1547 in an optimum way. Finally, the Q factor is related to oscillation time-response and initial phase. It is important to note that high values of Q make the detection difficult; in opposite, low values of Q may distort the oscillation severely. Similarly, a low BPF gain might prevent the detection while a high gain may result in unnecessarily high oscillation amplitude.

IV. EXPERIMENTAL RESULTS

In order to validate the above analysis, experimental results of the system of Figure 2 have been performed. The converter is a three-phase two-leg per phase operating from a 55V DC bus, output current about 1.6A and the switching frequency of 10 kHz. The IDA parameters are given in Table I and the others experimental platform parameters are given in Table II.

Figure 16 represents the DG operation without IDA connected to the grid. When the grid current is zero, the DG is islanded with the local load. It is demonstrated that a stable operation is also possible even if the grid is not connected, characterizing, in this way, an unintentional islanding operation. Furthermore, it can be noted an energy quality degradation when the DG is islanded with the local load.

On the other hand, Figure 17 demonstrates that by adding the IDA it is possible to have a stable operation when the grid is present and an oscillating operation whenever the DG operates in islanded mode; this validates the stability analysis carried out in section III. Note that after the grid is disconnected, there is an oscillation in the PCC voltage that has been predicted by the describing function of the saturation limiter to have amplitude of 7V and frequency of 12 Hz. This oscillation is seen in detail in Figure 18.

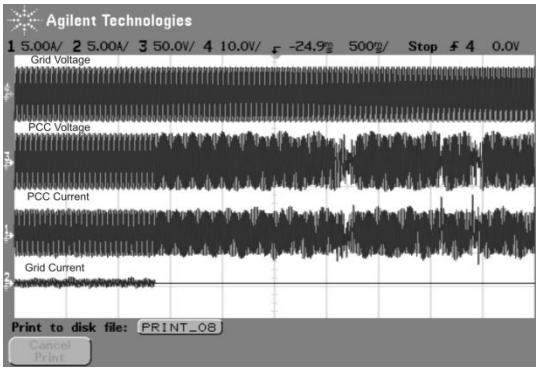

Figure 16. Experimental results without IDA - Grid Voltage, PCC Voltage, PCC Current and Grid Current when the grid is disconnected (islanded). Horizontal scale: Time (500ms/div). Vertical scale: Voltage (20V/div) and Current (2A/div)

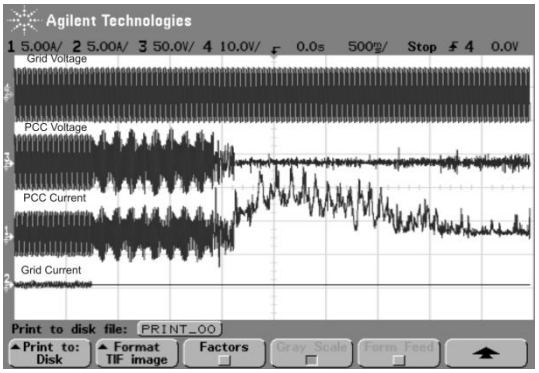

Figure 17. Experimental results with the IDA. From top to bottom: Grid Voltage, PCC Voltage, PCC Current and Grid Current when the grid is disconnected (islanded). Horizontal scale: Time (500ms/div). Vertical scale: Voltage (20V/div) and Current (2A/div)

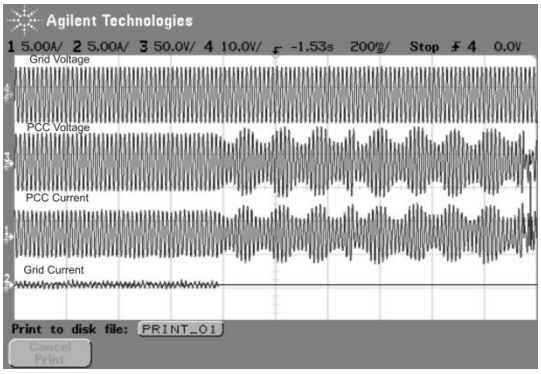

Figure 18. Experimental results with the IDA. From top to bottom: Grid Voltage, PCC Voltage, PCC Current and Grid Current when the grid is disconnected (islanded). Horizontal scale: Time (200ms/div). Vertical scale: Voltage (20V/div) and Current (2A/div)

V. CONCLUSIONS

This paper develops a stability analysis of a local Islanding Detection Algorithm (IDA) based on positive feedback technique that has no Non Detection Zone (NDZ). Its main attributes are its low cost and low impact on the voltage THD. A complete three-phase dynamic model of the system has been derived for the stability analysis. It demonstrated that a stable operation is possible even if the grid is not connected. In addition, by adding the IDA it is possible to have a stable operation if the grid is present and have an oscillating operation whenever the DG operates in islanded section, which allows detection. Furthermore, a modification on the IDA is proposed to improve the voltage amplitude oscillation profile during the islanding mode. Experimental results support the theoretical analysis carried out.

REFERENCES

[1] U.S. Department Energy, "International Energy Outlook – 2006", *available in http://www.eia.doe.gov*, June 2006.

[2] G. Celli, F. Pilo, "MV Network Planning under uncertainties on Distributed Generation Penetration", *IEEE on Power Engineering Society Summer Meeting*, July 2001.

[3] V. John, Z.Ye, A. Kolwalkar, "Investigation of Anti-Islanding Protection of Power Converter Based Distributed Generators Using Frequency Domain Analysis", *IEEE Transactions on Power Electronics*, Vol. 19, No. 5. p. 1177-1183, 2004.

[4] Std IEEE 1547, "Standard for interconnecting distributed resources with electric power systems.", *Institute of Electrical and Electronics Engineers*, 2003.

[5] Z. Ye, A. Kolwalkar, Y Zhang, P. Du and R. Walling, "Evaluation of anti-islanding schemes based on nondetection zone concept", *IEEE Transactions on Power Electronics*, p. 1171 – 1176, 2004 Vol. 19, NO. 5, 2004.

[6] Jun Yin, Liuchen Chang, Chris Diduch, "Recent Development in Islanding Detection for Distributed Power Generation", *Large Engineering systems Conference on Power Engineering*, LESCOPE-04, 2004.

[7] T. Funabashi, K. Koyanagi, R. Yokoyama, "A Review of Islanding Detection Methods for Distributed Resources", *IEEE Bologna PowerTech Conference*, Italy, 2003.

[8] O. Usta, M. A. Redfern, J. I. Barrett, "Protection of Dispersed Storage and Generation Units Against Islanding", *7th Mediterranean Electrotechnical Conference*, 1994.

[9] P. Mahat, Z.Chen, B. Bak-Jensen, "Review of Islanding Detection Methods for Distributed Generation", *IEEE Third International Conference on Electric Utilty Desregulation and Restructuring and Power Techonologies*, p.2743 – 2748, April 2008.

[10] S.R Samantaray, T.M.P.B.D. Subudhi, "A New Approach to Islanding Detection in Distributed Generators", *IEEE Third International Conference on Power Systems*, December 2009.

[11] J.H. Kim, J.G. Kim, Y.H. Kim, Y.C. Jung, C.Y. Won, "An Islanding Detection Method for a Grid-Connected System Based on the Goertzel Algorithm", *IEEE Trans. on Power Electronics*, Vol. 26, NO.4, April 2011.

[12] A. Gadheri, A. Esmaeilian, M. Kalantar, "A Novel Islanding Detection Method for Constant Current Inverter Based Distributed Generations", *IEEE 10th Conference on Environment and Electrical Engineering*, p.1 – 4, June 2011.

[13] Z. Ye, R. Walling, L. Garces, R. Zhou, L. Li, and T. Wang, "Study and Development of Anti-Islanding Control for Grid-Connected Inverters", Report of *National Renewable Energy Laboratory and General Electric Global Research Center*, New York, 2004.

[14] I. W. Jaskulski, H. Pinheiro, L. Mariotto, "Multi-Leg Voltage Source Converter for Grid Connected Wind Turbines", *International Conference on Clean Electrical Power*, ICCEP'07, Italy, 2007.

[15] R. F. Camargo, H. Pinheiro, "Synchronisation method for three-phase PWM converters under unbalanced and distorted grid", *IEE Proc.-Electr. Power Appl.*, Vol. 153, No. 5, September 2006.

[16] R. Cardoso, R. F. Camargo, H. Pinheiro, H. A. Gründling, "Kalman Filter Based Synchronization Methods", *37th IEEE Power Electronics Specialists Conference – PESC*,2006.

[17] J. Svensson, "Synchronisation Methods for Grid-Connected Voltage Source Converters", *IEE Proceedings – Gen. Transm. Distrib.*, Vol. 148, No.3, May 2001.

[18] Std IEEE 1547.1, "IEEE Standard Conformance Test Procedures for Equipment Interconnecting Distributed Resources with Electric Power Systems." *Institute of Electrical and Electronics Engineers*, 2005.

[19] K. Ogata, "*Engenharia de Controle Moderno*", Editora LTC, 1nd edição.

BIOGRAPHIES

Andrei Giordano Holanda Battistel: was born in 1987. He received his B.S. degree in Electrical Engineering from Federal University of Santa Maria in 2009 and his M.S. degree in Electrical Engineering from Federal University of Rio de Janeiro in 2011, where he is currently a PhD student. His research includes nonlinear systems, control theory applications and robotics.

Igor Weide Jaskulski was born in 1980. He received his B.Sc. of Electrical Engineering and M.Sc. degree from Federal University of Santa Maria, Brazil, in 2004 and 2007 respectively. Since 2007 he has been working with the Wind Power Industry in Germany. His main interests are wind turbine grid integration, modeling and simulation of power systems and power electronics and control associated with frequency converters connected to the grid.

Humberto Pinheiro: received the B.S. degree Electrical Engineering from Federal University of Santa Maria in 1983, the M.S. degree in Electrical Engineering from Federal University of Santa Catarina in 1987, and the PhD in Electrical Engineering from Concordia University, Canada, in 1999. Currently, he is associate professor at Electric Power Processing Department in Federal University of Santa Maria. His research interests include wind power systems and uninterruptible power supply systems.

APPENDIX

The sate equation of the grid connected inverter with the proposed anti-islanding algorithm is

$$\begin{bmatrix} \dot{x}_{BPF1} \\ \dot{x}_{BPF2} \\ \dot{x}_{PI1} \\ \dot{x}_{PI2} \\ \dot{i}^{d} \\ \dot{i}^{q} \\ \dot{v}^{d} \\ \dot{v}^{q} \\ \dot{i}_{L}^{d} \\ \dot{i}_{L}^{q} \\ \dot{i}_{g}^{d} \\ \dot{i}_{g}^{q} \end{bmatrix} = \begin{bmatrix} -\omega_n & -\omega_n^2 & K_{INV}K_I & 0 & K_{INV}K_P & 0 & 0 & 0 & -1 & 0 & 0 & 0 \\ 1 & 0 & 0 & 0 & 0 & 0 & 1 & 0 & 0 & 0 & 0 & 0 \\ 0 & 0 & 0 & 0 & 1 & 0 & 0 & 0 & 0 & 0 & 0 & 0 \\ 0 & 0 & 0 & 0 & 0 & 0 & 1 & 0 & 0 & 0 & 0 & 0 \\ 0 & 0 & -\frac{K_{INV}K_I}{L} & 0 & -\frac{K_{INV}K_P}{L} & 0 & \omega & 0 & 0 & -\frac{1}{L} & 0 & 0 \\ 0 & 0 & 0 & 0 & 0 & 0 & 0 & \omega & 0 & -\frac{1}{L_g} & 0 & 0 \\ 0 & 0 & 0 & -\frac{K_{INV}K_I}{L} & -\omega & -\frac{K_{INV}K_P}{L} & 0 & 0 & -\frac{1}{L} & 0 & 0 & 0 \\ 0 & 0 & 0 & 0 & 0 & \omega & 0 & 0 & -\frac{1}{L} & 0 & 0 & 0 \\ 0 & 0 & 0 & 0 & 0 & 0 & \frac{1}{C_L} & \frac{1}{C_L} & \frac{1}{RC_L} & -\omega & 0 & -\frac{1}{C_L} \\ 0 & 0 & 0 & 0 & \frac{1}{C_L} & \frac{1}{C_L} & 0 & 0 & \omega & -\frac{1}{RC_L} & -\frac{1}{C_L} & 0 \\ 0 & 0 & 0 & 0 & 0 & 0 & 0 & 0 & 0 & -\frac{1}{L} & 0 & \omega \\ 0 & 0 & 0 & 0 & 0 & 0 & 0 & 0 & \frac{1}{L} & 0 & -\omega & 0 \end{bmatrix} \begin{bmatrix} x_{BPF1} \\ x_{BPF2} \\ x_{PI1} \\ x_{PI2} \\ i^{d} \\ i^{q} \\ v^{d} \\ v^{q} \\ i_{L}^{d} \\ i_{L}^{q} \\ i_{g}^{d} \\ i_{g}^{q} \end{bmatrix} + \begin{bmatrix} 0 & 0 & K_{INV}K_P & 0 \\ 0 & 0 & 0 & 0 \\ 0 & 0 & 1 & 0 \\ 0 & 0 & 0 & 1 \\ 0 & 0 & \frac{K_{INV}K_P}{L} & 0 \\ 0 & \frac{1}{L_g} & 0 & 0 \\ 0 & 0 & 0 & \frac{K_{INV}K_P}{L} \\ \frac{1}{L_g} & 0 & 0 & 0 \\ 0 & 0 & 0 & 0 \\ 0 & 0 & 0 & 0 \\ 0 & 0 & 0 & 0 \\ 0 & 0 & 0 & 0 \end{bmatrix} \begin{bmatrix} v_g^{d} \\ v_g^{q} \\ i_{ref}^{d} \\ i_{ref}^{q} \end{bmatrix}$$

$$[\Delta v] = \begin{bmatrix} K\omega_n / Q & 0 & 0 & 0 & 0 & 0 & 0 & 0 & 0 & 0 & 0 & 0 \end{bmatrix} \cdot \begin{bmatrix} x_{BPF1} \\ x_{BPF2} \\ x_{PI1} \\ x_{PI2} \\ i^d \\ i^q \\ v^d \\ v^q \\ i_L^d \\ i_L^q \\ i_g^d \\ i_g^q \end{bmatrix}.$$